Full Length Research Paper

The groundwater geochemistry of the Saloum delta aquifer: Importance of silicate weathering, recharge and mixing processes

Serigne Faye[1]*, Mamadou Issa Ba [1], Moctar Diaw[1] and Seyni Ndoye[2]

[1]Department of Geology, Faculty of Science and Technology, University Cheikh Anta Diop (UCAD), P. O. Box 5005 Dakar-Fann, Senegal.
[2]Department of Civil Engineering, Ecole Supérieure Polytechnique, University Cheikh Anta Diop, Dakar, Senegal. BP 5085 Dakar Fann, Senegal.

The physical-chemical and isotopic characteristics of the groundwater in the Saloum detrital aquifer system obtained from a network of 74 sampling points have indicated the likely geochemical reactions and defined the groundwater flow regime in the context of a semi-arid region. The main geochemical zones with distinct water types and isotopic contents displayed through this investigation are the results of ion exchange reactions, both congruent and incongruent reactions of carbonate, silicate minerals combined with effects of recharge/ discharge by evaporation and salinization processes in the vicinity of the estuary system. Use of minor and trace elements against the conservative ions of Cl and Br supports the highly weathering processes of the aquifer matrix which seem even to affect by incongruent reactions the oxide and hydroxide minerals under aerobic conditions. In this region, recharge is highly heterogeneous and recent recharged waters as well as preferential flow paths have been evidenced using stable isotopes of ^{18}O and ^{2}H together with radioactive 3H.

Key words: Hydrochemistry, stable isotopes, radioactive isotope, groundwater recharge, salinization.

INTRODUCTION

Assessment and management of water resources for economic development are key issues due to damages caused by arid climate impact, increasing extraction for rural, pastoral and agricultural uses, and poor protection policies. These impacts are particularly perceived in the coastal sahelian band during the prolonged drought of the 1970's which consequently caused continuous lowering of the water table, increasing abstraction cost and progressive water quality deterioration and salinization (Richter and Kreitler, 1993).

On the other hand, the naturally occurring processes that influence and generate the ultimate groundwater chemistry constitute another important aspect to viably ensure irrigation and domestic water use, and may provide a model for improving effective groundwater resource management and protection (Edmunds et al.,

2002). In fact, they can reveal modifications of the initial baseline water chemistry and more importantly augment our knowledge on the recharge, the sources and spatial variability (Edmunds and Walton, 1980; Adar and Neuman, 1988) as well as rates of groundwater flows, discrete groundwater pathways, mixing and relative residence times (Lee and Krothe, 2001; Uliana and Sharp, 2001).

Since 2000, a detailed hydrochemical study of the Saloum hydrosystem (Senegal) was initiated in order to develop a clear understanding of the salinization processes with special emphasis made on the sources, mechanism and magnitude of the saltwater intrusion. Currently, the groundwater resource is constrained by occurrence of moderate to high salinity in the northern and western parts of the aquifer inferred by the hyper saline Saloum River (Faye et al., 2003, 2005). In this present study, a multi-parametric method based on an extensive chemical (major, minor and trace elements) and isotopic (^{18}O, ^{2}H and ^{3}H) dataset is used to

---

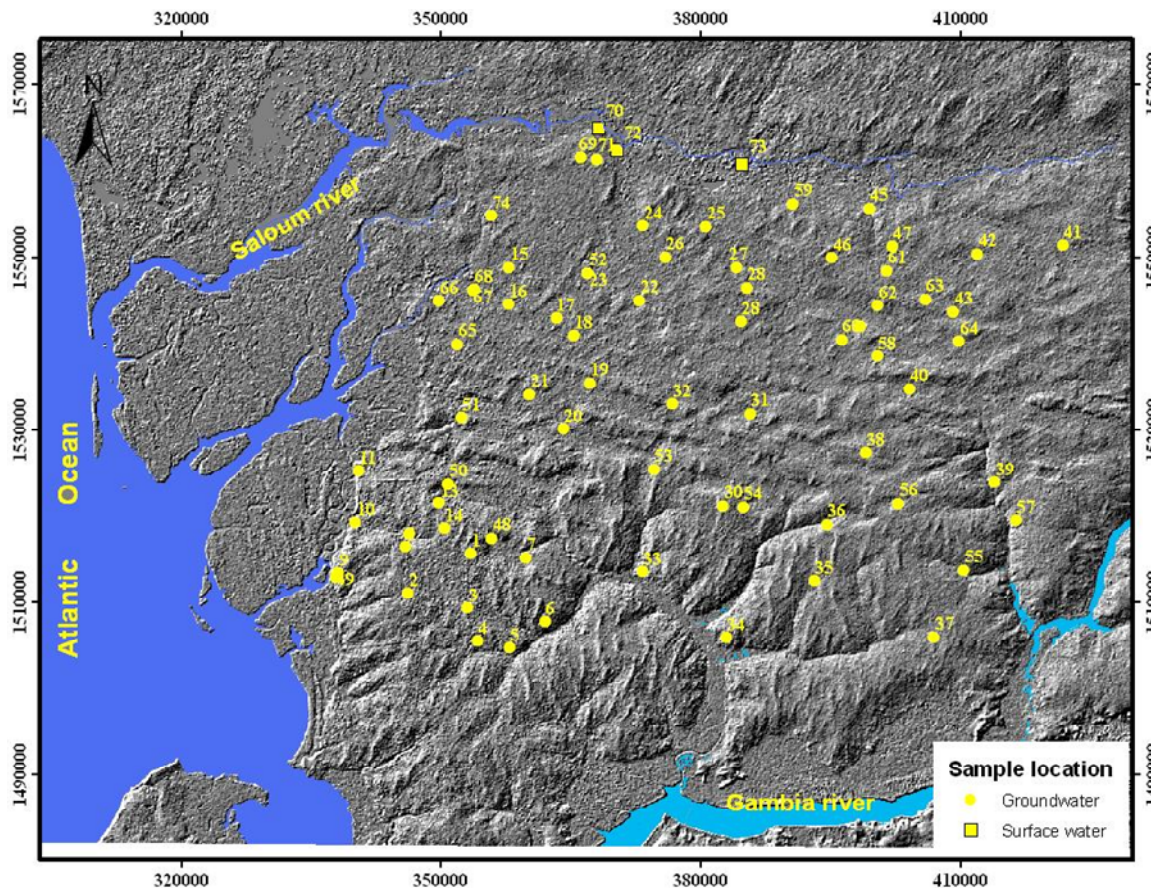*Corresponding author. E-mail: serigne_faye@yahoo.com.

Figure 1. Location of the study area and sampling network.

characterize the importance of weathering processes and to improve our conception of the groundwater flow regime in relation to the importance and distribution of recharge, mixing and relative residence times. This is of prime importance in the Saloum delta region which superficial groundwater stored in the Continental Terminal (CT) formations constitutes a unique accessible resource for domestic and pastoral water supply.

Geological and hydrogeological settings

The study area (Figure 1) comprises the southern part of the Saloum River catchment which is a low lying inverse estuary and extends towards the plateau zone located inland at +40 m altitude (Diop, 1986). To the north, it is bounded by the Saloum River and the western limit is marked by the Atlantic Ocean. The region is characterised by a "soudano-sahelian" type climate with mean monthly temperatures between 25 to 32°C, mean precipitation between 600 to 800 mm and potential evapotranspiration from 1 900-2 400 mm/year. Water loss through this intense evaporation is the main cause of the hyper salinization (from the 36.7% at the river mouth to 90% at Kaolack) of the Saloum River and

accumulation of halite crusts in the flat-lying alluvial deposits within the drainage basin.

The sedimentary deposits are mainly composed of the CT formations overlain by thin and younger quaternary sand (5 m) and alluvial deposits in the river bed. The CT sediments are Cenozoic (Oligo-Miocene to Pliocene) detrital marginal marine origin; they present evidence of an intense ferralitic alteration during the late Miocene period with formation of ferruginous concretions, crusting, neoformation of kaolinite and silica movement (Lappartient, 1985; Conrad and Lappartient, 1987). The sediments with a variable thickness from 10 m in the NNW to 80-100 m eastward (Diluca, 1976) include discontinuous interbedded sand, sandstone, sandy clay, clayey sand, silt and clay, with marine macrofossils depo-sited in the littoral environment; they are locally indurated and clay veined sandstone beds and ferruginous crusting at the top formation. The unconsolidated sediments are predominantly fine grained sands which are coated by micritic (10 to 20 μm) to sparitic (100 μm) calcite at depth (Lappartient, 1985) in the eastern part of the region. Glauconite is also found at 30 to 40 m depth. In the ferruginous sand horizon, Fe-oxides (goethite) and hydroxides (hematite) form the cement of the quartz grains; goethite being more abundant than hematite.
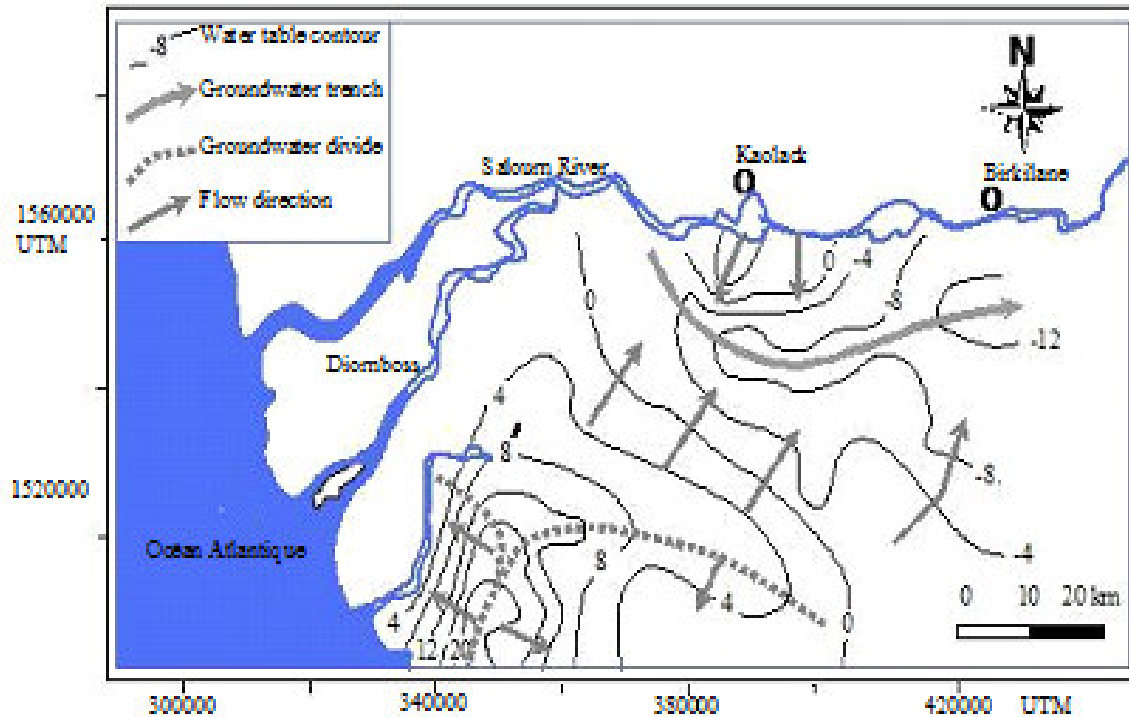
Figure 2. Potentiometric surface map (in metre) of November 2003.

From the hydrogeological point of view, the aquifer consists of the CT formations lying unconformably on an impervious Eocene substrate composed of marl, indurate limestone and clay with variable altitude between -100 and -20 m. Transmissivity vary between 3×10^{-4} and 3.5×10^{-2} m²/s and hydraulic conductivity between 1.7×10^{-5} and 2.2×10^{-3} m/s.

Water table depth varies from less than 3 m in the West to 30 m towards East. Piezometric head distribution show the same pattern since 1976; it is characterized by two main features (Figure 2): A NNE-SSW oriented groundwater mound (head>20 m) located in the plateau zone (40 m altitude) and a groundwater trench (characterized by a high hydraulic conductivity values) with head below mean sea level (down to –12 m) which collects part of the flow derived from the groundwater mound and flow from the Saloum River. In the southern part of the system, groundwater flow is divergent and discharges respectively to the Bandiala branch (a tributary of the Saloum River system) and to the Djokoye (a tributary of the Gambia River). Despite the lack of temporal record of the head measurements, some variability is noticed with the two datasets (dry season 2000 and rainy season 2003) where head changes can be up to 4 m rise in the South.

FIELD AND ANALYTICAL METHODS

During the course of this program, two field campaigns (in April

2000 and November 2003) were carried out at a network of sampling stations within the limits of the system. However, for the present paper, we focus mainly on the second sampling campaign which covers a network of 71 wells complemented by 3 river water sampling (Figure 1) and concerns a more complete set of analytical data comprising major, minor and trace elements, and isotopes. Well geographical locations, field measurements and samples collection were carried out on site at the well head according to standard methods (Greenberg et al., 1992). The pH, water temperatures and electrical conductivity (EC) were measured on site using WTW Multiline F/SET-3 Kit, and the total alkalinity (as HCO_3) was determined by titration with 0.01 or 0.1 HCl against methyl orange and bromocresol green indicators. Prior to sampling and field measurements, depths to water table were recorded. Samples for analysis of inorganics were 0.45 μm filtered into an acid-washed polyethylene bottles, one aliquot being acidified to pH less than 2 by addition of high purity HNO_3 for analysis of cations and trace elements. Another unacidified water samples were collected and coolly conserved for stable isotopes and tritium analyses. All samples analyses were performed at the Institute of Groundwater Ecology (IGE) /GSF Research Center/Munich/Germany.

Major cations and anions in the water samples were measured on a Dionex ion chromatography (IC Dionex 100), whereas fluoride and bromide were analysed using Dionex ion chromatography (IC Dionex 500) according to the established procedures at the IGE.

The following elements Sr, B, Si, Fe_{total}, Ba, Li, Mn, Zn, Cu, Ni, Cd, Co, Cr, and Pb were analysed by inductively coupled plasma-atomic emission spectrometer (ICP-AES) using a Liberty 200AX-Varian type on samples that had been filtered through 0.45 μm filters and acidified to pH less than 2 using 16N pure HNO_3.

Hydrogen and oxygen isotopes analysis were performed by respectively employing the standard CO_2 equilibration (Epstein and Mayeda, 1953) and the zinc reduction techniques (Coleman et al., 1982), followed by analysis on mass spectrometer. All oxygen and

hydrogen isotopes analysis are reported in the usual δ notation relative to Vienna- Standard Mean Oceanic Water (V-SMOW) standard. Typical precisions are ±0.1 and ±1.0% for the oxygen and deuterium, respectively. Tritium analyses were performed by electrolytic enrichment and liquid scintillation counting method (Thatcher et al., 1977). ^3H concentrations are expressed in tritium units (TU) and the detection limit is 0.7 TU.

RESULTS AND DISCUSSION

Geochemical patterns

The principal characteristics of the surface and groundwaters are shown in Table 1. The majority of the groundwater samples have pH values which range between 5.1 and 11.5, while temperatures varied from 24.7 to 35.3°C, consistent with the shallow nature of the aquifer system. The EC values commonly increase dramatically from the central and eastern portions of the aquifer (35 µS/cm as minimum) towards the delta system vicinity (4,920 µS/cm as maximum) where the Saloum hypersaline river exhibits in 3 sampling sites EC values between 78,300 and 90,100 µS/cm.

Most of the freshwaters are dominated by Na (39 to 88% meq) or Ca (41 to 84% meq) of the cations and by Cl (≥ 36% meq) or mostly HCO_3 (40 to 91% meq) at the exception of the polluted groundwater samples which exhibit high NO_3 contents (up to 987 mg/l). These relative occurrences of both cations and anions in the groundwater samples give a wide range of hydrochemical types from Na-HCO_3, Na-Cl, Na-HCO_3/Cl, Ca-HCO_3, Ca/Na-HCO_3 to Na/Ca-Cl (Table 1). Spatial distribution of these hydrochemical types shows occurrence of Ca-HCO_3 waters towards the east and northeast of the region, while Na-HCO_3, Na/Ca-HCO_3 and Ca-HCO_3 waters occur in the south western part of the aquifer. Assuming that these waters were recharged from the south eastern part of the aquifer, water types with lower mineral content can be interpreted as the first step of water-rock interactions occurring in dilute solutions where the process of constant exchange of Ca for Na is taking place to give mild mineralisation towards the flow direction. During the processes, HCO_3 is subsequently replaced by Cl and Na increases regularly leading thus to Na-Cl groundwater type down gradient flow through cation exchange reactions. As Cl concentrations increase to reach 85% meq of the anions, all the saline ground-waters in our data set are Na-Cl, Na/Ca-Cl with one sample located close to the mangrove ecosystem zone exhibiting Na-SO_4/Cl water type (where the sulphate enrichment is probably due to intrusion of evaporated surface water bodies).

To determine the hydrochemical processes in the Saloum detritic aquifer which may occur both in the fresh and saline groundwaters, the concentration of the various cations to chloride ratios are presented as a function of the chloride contents or Cl/Br ratios used as conservative against which the water-rock interaction can be inferred.

The relationship between ions/Cl and Cl (Figure 3) are valuable for assessing the source and mineralization in the Saloum groundwater. As shown in Figure 3a (Cl *vs.* Na/Cl), the high Na/Cl molar ratio (up to 6 to 7) in the fresh groundwater is indicative of a strong water-rock interaction and may be explained by the Na being derived predominantly from weathering and/or cation exchange reactions.

In the saline groundwater where the ratio is below the seawater value (0.86), Na depletion is most likely due to the adsorption reaction by clay mineral, which is a common process in salinized areas (Ghassemi et al., 1995). Variations of the other cations/Cl ratios vs. Cl con-centrations (Figures 3b, c and d) are similar to the Na/Cl *vs.* Cl trend which support the model discussed above where the chemistry of the low salinity groundwater is controlled by water-rock interaction.

There is some correlation between Ca-HCO_3 concen-tration (Figure 4b) in some wells; and the groundwater in these wells are generally saturated with respect calcite (log SI from -3.9 to +4.0) (Table 1), suggesting that calcite dissolution is a somewhat a major process. Whereas, no correlation was found between Ca and SO_4 concentrations and the low SI with respect to gypsum (log SI < 0) militates against gypsum dissolution as a major source of Ca. The Ca ions would rather probably be derived from calcite dissolution and/or feldspar minerals weathering. But since feldspar and mica minerals were not identified as components of the matrix reservoir, Ca derived from weathering of these silicates can not be presently promoted as major geochemical sources. Moreover, strong silicate weathering processes produce high aqueous silica concentrations which when plotted against Cl (Figure 4a) should confirm the importance of these reactions in controlling the cations concentrations in the groundwaters. Groundwater samples are undersaturated with respect to amorphous silica (log SI between –2.96 and –0.17), indicating that precipitation of amorphous silica does not limit silica concentrations. At low temperatures, SI would be largely derived from silica weathering reactions rather than quartz dissolution and the precipitation of amorphous silica is inhibited by kinetic constraints. These processes of bases exchanges reactions, silicate weathering and calcite precipitation/dissolution are superimposed by input of the saline water mixing in the saline groundwater group.

Minor and trace elements

A wide range of minor and trace elements have been investigated to shed further light on the geochemical processes occurring in the highly weathered reservoir of the CT formations; these elements (Table 2) will pre-sumably augment evidence provided by analysis of the major ion chemistry. Below we briefly describe the trends observed within the groundwater samples.

Table 1. Major ions characteristics of water samples (SI: Saturation Index, Cal. Calcite, Qtz: quartz, Gyp: gypsum, Dol: dolomite, Str: strontianite, Cel: celestite).

N°	Depth (m)	pH	T (°C)	Cond (uS/cm)	Na	K	Mg	Ca	Cl	HCO₃	SO₄	NO₃	Water types	Cal	Qtz	Gyp	Dol	Str	Cel
										mg/l						SI			
1	24.26	6.2	29.1	445	34.7	3.1	11.4	26.5	28.7	61.0	0.4	159.7	Na-HCO₃	-1.9	-1.5	-4.3	-4.0	-3.3	-4.5
2	14.22	6	29.5	97	15.6	1.0	1.2	5.0	6.6	39.7	0.1	39.3	Na-HCO₃	-3.0	-1.7	-5.3	-6.3	-4.8	-5.9
3		5.9	30.2	59	6.7	0.4	0.5	8.9	3.1	61.0	0.2	2.4	Na-HCO₃	-2.6	-1.6	-4.9	-6.2	-5.1	-6.1
4		6.2	28.6	231	47.1	1.1	0.2	6.6	24.6	79.3	0.3	76.7	Na-HCO₃	-2.4	-1.6	-5.0	-6.0	-4.2	-5.5
5	13.75	5.1	29.7	438	80.2	0.5	2.4	5.1	37.4	33.6	0.2	150.6	Ca-HCO₃	-4.0	-1.6	-5.3	-8.0	-5.3	-5.3
6	19.12	6.2	29.1	126	23.8	1.4	0.2	3.8	5.8	85.4	0.2	49.6	Na-HCO₃	-2.6	-1.6	-5.5	-6.2	-4.3	-5.9
7	12.18	6.1	29.2	68	9.3	1.1	0.7	3.9	4.8	21.4	0.1	20.4	Na-HCO₃	-3.2	-1.4	-5.6	-6.9	-4.9	-6.0
8	8.58	6.1	28.6	148	12.3	0.4	0.0	20.3	6.5	94.6	0.9	10.9	Na-HCO₃	-1.9	-1.5	-3.9		-3.8	-4.5
9	2.8	6.7	29	120	7.6	0.2	0.6	14.6	10.2	79.3	0.4	25.1	Ca-HCO₃	-1.5	-1.6	-4.4	-4.1	-3.6	-5.2
10	1.95	5.3	28.3	1653	168.9	61.9	29.9	139.7	174.0	61.0	368.7	86.9	Na/Ca-SO₄	-2.3	-1.4	-1.0	-5.0	-4.1	-1.5
11	7.03	6.6	28.3	1686	236.8	7.7	3.3	221.6	474.7	119.0	21.4	2.3	Na/Ca-Cl	-0.4	-1.1	-1.9	-2.4	-2.6	-2.8
12	5.12	6.2	28.6	518	55.5	2.0	6.4	37.1	60.6	61.0	4.1	113.3	Na-Cl	-1.8	-1.1	3.2	-4.1	-3.4	-3.5
13	15.73	6.6	29.6	62	10.6	0.4	0.4	4.2	2.5	33.6	1.5	15.7	Na-HCO₃	-2.5	-1.1	-4.3	-5.7	-4.2	-4.8
14		6.8	29.2	184	38.2	0.3	0.8	3.8	16.6	103.7	0.1	77.4	Na-HCO₃	-1.9	-1.2	-5.7	-4.2	-3.4	-5.9
15	7.77	6.3	28.7	1333	129.3	13.0	22.3	115.6	232.8	39.7	1.3	397.0	Na/Ca-Cl	-1.5	-1.1	-3.4	-3.4	-3.0	-3.7
16		6.1	29.4	611	31.2	19.3	17.7	46.5	54.1	27.5	5.1	199.7	Na-Cl	-2.2	-1.1	-3.0	-4.5	-3.8	-3.4
17	9.61	6.9	29.9	384	39.8	1.1	1.5	41.1	37.9	100.7	1.3	59.7	Ca-HCO₃	-0.8	-1.1	-3.6	-2.8	-3.0	-4.5
18	11.37	6.8	29	248	28.8	0.9	3.4	22.3	24.2	76.3	0.5	30.5	Ca-HCO₃	-1.3	-1.2	-4.2	-3.1	-3.0	-4.7
19	18.07	6.4	28.8	132	14.7	1.1	1.9	8.9	16.4	54.9	0.2	7.4	Na-HCO₃	-2.2	-1.1	-4.9	-4.7	-3.9	-5.4
20		5.8	28.4	213	34.3	1.5	1.9	3.9	22.8	21.4	0.1	72.8	Na-Cl	-3.6	-1.1	-5.6	-7.2	-4.9	-5.7
21	14	6.4	28	293	37.2	0.8	3.6	18.7	31.5	39.7	0.2	87.6	Na-Cl	-2.1	-1.0	-4.7	-4.5	-3.7	-5.1
22	14.16	7.8	28.9	1013	114.5	2.2	6.5	102.9	216.4	158.6	3.7	49.3	Na/Ca-Cl	0.6	-1.2	-2.9	0.3	-1.6	-3.9
23	6.27	7.6	28.1	1885	236.3	7.7	30.8	141.0	497.7	122.0	2.0	30.1	Na-Cl	0.4	-0.9	-3.1	0.4		-3.3
24	7.77	7.3	29.3	4920	791.7	31.3	106.3	189.8	1498.6	51.9	78.2	259.5	Na-Cl	-0.3	-0.7	-1.7	-0.5	-1.7	-1.8
25	10.48	7.1	28.3	2400	359.2	10.0	29.2	98.1	624.6	91.5	40.4	63.0	Na-Cl	-0.4	-0.7	-2.0	-1.1	-2.0	-2.4
26	16.32	7.3	30.1	495	66.2	6.1	15.9	72.0	208.8	64.1	1.0	63.8	Na/Ca-Cl	-0.4	-1.0	-3.6	-1.2	-2.1	-4.0
27	16.32	7.7	30.2	495	20.5	1.0	6.2	92.8	28.2	268.4	0.9	3.4	Ca-HCO₃	0.8	-1.1	-3.5	0.6	-1.6	-4.5
28	26	7.7	30.1	594	34.9	1.9	6.2	93.4	75.3	225.0	0.8	1.7	Ca-HCO₃	0.7	-1.0	-3.5	0.5	-1.5	-4.4
28	22.94	7.1	29.2	282	18.0	2.8	5.3	37.5	18.2	146.4	1.4	9.5	Ca-HCO₃	-0.5	-0.9	-3.6	-1.5	-2.4	-4.2
30	33.05	7.7	29.8	85	14.6	0.5	0.2	8.6	6.2	76.3	0.3	11.6	Na-HCO₃	-0.7	-1.0	-4.8	-2.8	-2.5	-5.2
31		8.5	29.7	318	12.1	2.6	1.9	56.0	6.8	195.2	4.0	4.9	Ca-HCO₃	1.2	-0.9	-3.0	1.3	0.0	-2.9
32	16.76	7.2	29.8	181	20.4	0.6	2.9	13.3	20.7	30.5	0.1	51.8	Na-Cl	-1.5	-0.9	-5.1	-3.3	-3.2	-5.6
33	5	7.6	28.6	398	36.5	26.4	7.9	21.5	52.1	54.9	7.9	72.4	Na-Cl	-0.7	-1.2	-3.1	-1.5	-2.4	-3.6
34	16.02	7.8	29.4	114	22.4	0.5	0.3	4.0	9.1	42.7	0.2	38.4	Na-HCO₃	-1.2	-1.2	-5.3	-3.3	-2.9	-5.7
35	22.55	7.7	29.8	254	17.9	0.9	3.6	27.7	23.3	88.5	0.3	80.5	Ca-HCO₃	-0.2	-0.9	-4.4	-1.1	-2.1	-5.0

Table 1. Continued.

36	21.33	7.9	29	280	23.9	3.4	7.3	20.9	26.1	76.3	0.2	85.6	Ca-HCO₃	-0.2	-1.2	-4.7	-0.6	-1.7	-4.9
37		7.4	30.1	61	7.0	0.6	1.3	4.7	5.4	85.4	0.3	4.2	Na-HCO₃	-1.2	-1.2	-5.0	-2.8	-3.2	-5.7
38	36.96	10	27.6	35	2.4	0.5	0.1	5.1	1.4	39.7	0.2	2.5	Ca-HCO₃	1.0	-1.5	-5.1	0.8	-0.8	-5.6
39	19.3	8.9	31.2	389	8.4	0.7	3.9	75.6	8.3	198.3	11.4	7.4	Ca-HCO₃	1.8	-1.2	-2.4	2.5	-0.8	-3.7
40	27.47	9.6	30.3	79	11.3	1.2	0.2	5.5	9.1	61.0	0.3	10.8	Ca-HCO₃	0.9	-1.2	-5.0	0.5	-0.8	-5.4
41	37.01	9.2	30.6	286	14.1	0.8	7.1	41.3	19.3	192.2	1.4	7.8	Ca-HCO₃	1.8	-1.2	-3.5	3.1	0.0	-4.1
42	30.35	10.6	29.3	358	21.4	1.4	3.5	50.8	36.4	134.2	0.9	15.3	Ca-HCO₃	3.1	-1.9	-3.6	5.4	1.2	-4.3
43	32.14	10	30.5	655	25.4	1.2	7.4	106.3	68.3	289.8	1.5	1.9	Ca-HCO₃	3.1	-1.6	-3.2	5.4	0.8	-4.3
44	23.03	9.6	30.4	364	21.4	2.6	7.2	53.7	23.1	167.8	1.1	29.2	Ca-HCO₃	2.2	-1.4	-3.6	3.9	0.2	-4.3
45	9.29	9.7	29.7	2220	273.3	14.4	61.1	143.6	395.7	30.5	19.1	515.0	Na-Cl	1.9	-1.3	-2.3	3.6	0.2	-2.6
46	26.62	10.6	29.5	299	13.2	0.8	0.0	35.9	30.9	131.2	1.1	5.9	Ca-HCO₃	3.0	-2.0	-3.7	1.2	0.6	-4.1
47	21.58	10.2	29.8	1496	151.8	1.9	17.7	148.0	376.9	61.0	0.5	56.2	Na/Ca-Cl	2.7	-0.2	-3.7	4.8	0.9	-4.2
48		5.2	29.4	267	24.4	4.6	6.5	12.0	23.0	24.4	0.4	84.7	Na-Cl	-3.6	-1.2	-4.6	-4.3	-4.7	-4.4
49		6.3	28.4	3390	284.3	66.4	33.6	400.1	442.4	115.9	49.1	987.7	Na/Ca-Cl	-0.6	-1.2	-1.6	-2.0	-2.5	-2.2
50		5.1	27.2	716	52.7	22.1		40.5	71.2	21.4	1.3	238.1	Na-Cl	-3.4	-2.6	1.2		-5.2	0.7
51		5.3	25	224	20.3	1.0	5.0	57.0	43.2	125.1	2.3	13.7	Na-HCO₃	-2.2	-1.1	-3.2	-5.2	-4.3	-4.1
52		8.2	30.4	391	12.7	1.3	5.8	69.5	12.9	241.0	0.6	9.3	Na-Cl	1.1	-1.1	-3.7	1.4	-1.3	-4.8
53		7.5	30.2	76	10.1	1.7	0.6	7.1	7.8	39.7	0.3	11.9	Na-HCO₃	-1.3	-1.1	-4.8	-3.4	-3.3	-5.5
54		7.7	28.9	118	12.1	1.2	2.1	13.1	5.0	73.2	1.6	0.4	Ca-HCO₃	-0.6	-1.0	-3.9	-1.7	-3.3	-5.3
55	19.47	7.6	29.1	234	24.5	1.1	5.6	14.6	15.4	61.0	0.2	98.4	Ca-HCO₃	-0.8	-1.1	-4.8	-1.7	-2.3	-5.1
56		8.6	24.7	109	4.4	0.7	1.2	17.4	3.5	67.1	0.5	0.2	Ca-HCO₃	0.3	-1.1	-4.2	-0.1	-2.2	-5.5
57		8.4	28.7	248	15.4	1.2	1.7	35.9	8.4	115.9	9.3	34.1	Ca-HCO₃	0.7	-1.0	-2.8	0.4	-0.8	-3.0
58		11.5	35.3	1826	454.9	14.1	4.1	5.0	332.2	396.5	59.9	0.9	Na-Cl	3.5	-3.0	-3.0	7.0	2.2	-2.9
59	10.89	10.3	28.5	2200	367.4	23.3	42.6	63.2	563.7	97.6	33.7	138.5	Na-Cl	2.6	-1.6	-2.3	5.4	1.1	-2.5
60		11	29.4	522	14.3	0.8	10.3	86.6	24.4	265.4	1.7	17.9	Ca-HCO3	4.0	-2.3	-3.2	7.4	2.1	-3.9
61		8.4	30.5	748	60.5	2.0	0.0	87.5	191.1	97.6	0.6	18.8	Na/Ca-Cl	1.0	-1.0	-3.7		-1.3	-4.6
62		9.2	30.2	327	28.2	2.5	6.5	31.8	31.5	106.8	1.8	43.4	Ca-HCO₃	1.4	-1.1	-3.5	2.4	-0.3	-4.0
63		7.5	30.1	257	28.2	1.0	4.6	20.8	35.0	61.0	0.5	29.6	Ca-HCO3	-0.7	-1.0	-4.2	-1.8	-2.4	-4.7
64		7.6	30.4	148	8.3	2.1	3.6	19.5	9.8	91.5	0.6	4.3	Ca-HCO₃	-0.4	-1.0	-4.1	-1.3	-2.2	-4.6
65		6.8	28.4	139	8.2	0.7	1.4	27.3	5.5	94.6	1.3	0.9	Ca-HCO₃	-1.1	-0.8	-3.7	-3.1	-2.9	-4.2
66		7.2	28.3	704	44.2	14.2	6.4	94.4	69.2	204.4	7.6	81.3	Ca-HCO₃	0.1	-1.0	-2.6	-0.7	-1.7	-3.1
67		7.4	27.9	2930	180.7	15.3	0.0	489.0	701.6	244.0	2.7	308.5	Na/Ca-Cl	0.9	-0.9	-2.7		-1.6	-4.0
68		6.1	29.6	995	111.6	1.2	7.1	99.5	266.3	27.5	0.3	55.2	Na-Cl	-1.8	-0.7	-4.0	-4.6	-4.0	-4.8
69		5.9	29.7	571	54.9	0.7	10.5	43.0	136.3	24.4	0.3	50.9	Na-Cl	-2.4	-0.7	-4.2	-5.2	-4.1	-4.6
70		8.5	28.8	79000	13060	707.3	2445.0	692.6	18920.0	192.2	4657.5	6.1	Na-Cl	1.6	0.3	0.9	3.8	0.7	3.0
71		5.1	29.6	1516	262.3	6.6	10.4	36.8	413.1	24.4	6.1	21.1	Na-Cl	-3.3	-0.6	-3.1	-7.0	-4.8	-3.3
72		9.1	28.6	78300	12489	727.7	2365.3	790.1	17526.0	253.3	4691.4	12.7	Na-Cl	2.4	-0.2	0.4	5.4	1.4	2.5

Table 1. Continued.

| 73 | 7 | 29 | 90100 | 16020 | 782.4 | 2716.5 | 852.2 | 23220.0 | 396.5 | 5389.7 | 15.0 | Na-Cl | -0.4 | -0.1 | 0.5 | 8.2 | -0.5 | 2.6 |
| 74 | 7 | 29 | 1208 | 132.7 | 2.7 | 22.1 | 106.1 | 323.6 | 122.0 | 6.1 | 2.0 | Na-Cl | -0.3 | -0.5 | -2.7 | -1.0 | | |

Halogens (Br, Cl and F)

Among the halides, the chemically similar ions of Cl and Br are the most conservative in aqueous phase; they are particularly good indicators for seawater intrusion (Arad et al., 1986; Richter and Kreitler, 1993; Dror et al., 1999). The diagram Cl vs. Br (Figure 4c) of the groundwater samples evidences the unique marine source of both ions in the groundwater samples at the exception of two well samples exhibiting lower Br/Cl ratio values which are presumably induced by human and especially pastoral activities around the well head.

The fluoride F concentrations are not easy to explain; common hypothesis for F suggest;(1) mixing with deep groundwater; (2) dissolution of F bearing minerals; (3) high evapotranspiration in arid area; (4) clays rich F aquitards (Agrawal et al., 1997) ; (5) dissolution of traces carbonate and 6/ ion exchange reactions. In the groundwater samples, F concentrations are generally low (< 1 mg/l) except in four wells which exhibit values ranging between 2 and 64.6 mg/l. The low F content of most of the groundwater samples and the relatively constant F/Cl ratio as Cl increases suggests that the source of Cl is different to that for F. In addition there is no F-rich minerals, neither other important contribution from water-rock interaction and a known external source of groundwater that could promote large distribution of high F occurrence in the groundwater samples. The low F concentrations in the saline ground-water further indicate that direct recharge and subsequent evaporation occur in this area.

Whereas, the highest F concentrations (55 and 64 mg/l) found in the two least saline groundwater wells located at shallow depth at the vicinity of the Saloum River could be the result of the combined effects of evaporation, calcite dissolution and ion exchange reactions. But it seems that aridity of climate is the primary factor since high F groundwaters are located in low lying area at shallow depth.

Alkaline and alkaline earth trace elements (Sr and Li)

Besides the Sr delivered via atmospheric aerosols dissolved in rainfall and dry dust fallout, the Sr released from minerals (silicate and carbonate) during weathering within the soil zone and the aquifer is the most likely process occurring in the Saloum CT aquifer. It is though that these processes occur at the initial stage of the groundwater chemical evolution in this system. In addition in the saline groundwater group, the poor correlation between Sr and Cl (Figure 4d) indicates that an additional input of Sr occurs. In fact Sr/Cl even Li/Cl molar ratios are different to those expected from simple mixing with seawater. Input derived from Sr bearing minerals (celestite and strontianite) is ruled out since these minerals are not encountered in the aquifer matrix. The relationships between Sr and Ca and between Sr and HCO_3 (Figures 5a and b) suggest that the origin of Sr in the groundwater cannot be explain by dissolution of carbonate minerals alone although a quite positive correlation is observed between Ca and Sr but it is poor between Sr and HCO_3. By using the relationship between excess (Na+K) and the dissolved Sr, it is possible to see weather silicate (feldspar and micas) weathering is involved as input of dissolved Sr. As shown in Figure 5c, the excess (Na+K) value of the fresh groundwater around 1 as Sr increases is an indication that feldspar and mica weathering is not a likely process in the system. This trend emphasizes the importance of other process involved in addition to the role of carbonates dissolution in the Sr budget of the groundwater. Exchange through adsorption and desorption is almost certainly important, as evidenced by the relatively high Sr concentrations in the low-Na waters, and the general similarity of the Sr and Ca vs. Cl plots.

Lithium is know to be a good indicator of water-rock interactions since it is not rapidly removed from solution in secondary minerals and also the ion is a reliable indicator of groundwater residence times (Edmunds and Smedley, 2000). Sources of Li concentration in groundwater may be derived from minerals such as micas, feldspars and clays, and also from evaporates and saline waters. Clay minerals greatly infer in its concentration due to the fact that Li can replace Fe and Mg ions in the clay lattices. The lithium concentrations (range: 1-109 µg/l) display the same trends (Figure 5d) as Sr and K. It appears to be affected by ion exchange reactions; this may be due to the ease with which Li is displaced from exchange sites of the clay minerals by Na and K. Also, Darling and Edmunds (1987) suggested an adjustment of the Mg-rich clays by rejecting Li.
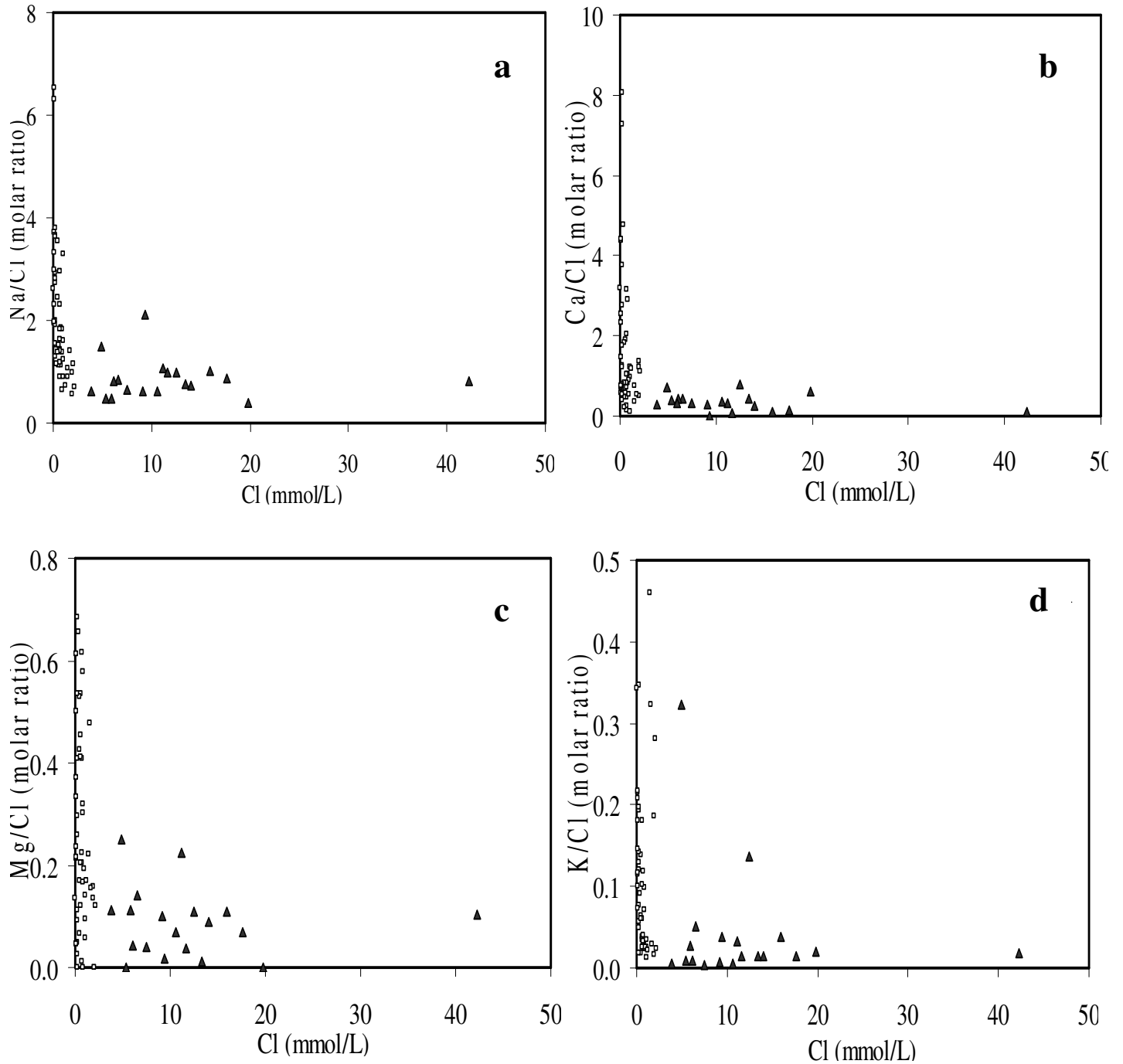
Figure 3. Major ions molar ratios (a) Cl *vs.* Na/Cl, (b) Cl *vs.* Ca/Cl, (c) Cl *vs.* Mg/Cl, (d) Cl *vs.* K/Cl, (empty square: fresh groundwater; filled triangle: saline groundwater).

Other minor and trace elements (B, Ba, Fe, Mn, Zn, Ni, Cd, Cr, Pb, Cu)

Boron occurrence in the water samples has been largely discussed previously (Faye et al., 2005) to analyse salinization processes in the Saloum delta system. Its concentration varies between 7 and 139 µg/l in the freshest groundwaters and between 13 and 650 µg/l in the saline groundwater group. Boron concentrations are markedly lower in the low-Na saline groundwaters, which strongly suggests that sorption is occurring after the salinization processes (freshening). Also, it is known that both oxyhydroxides and clay minerals infer on the B concentrations by sorption process, but still the actual
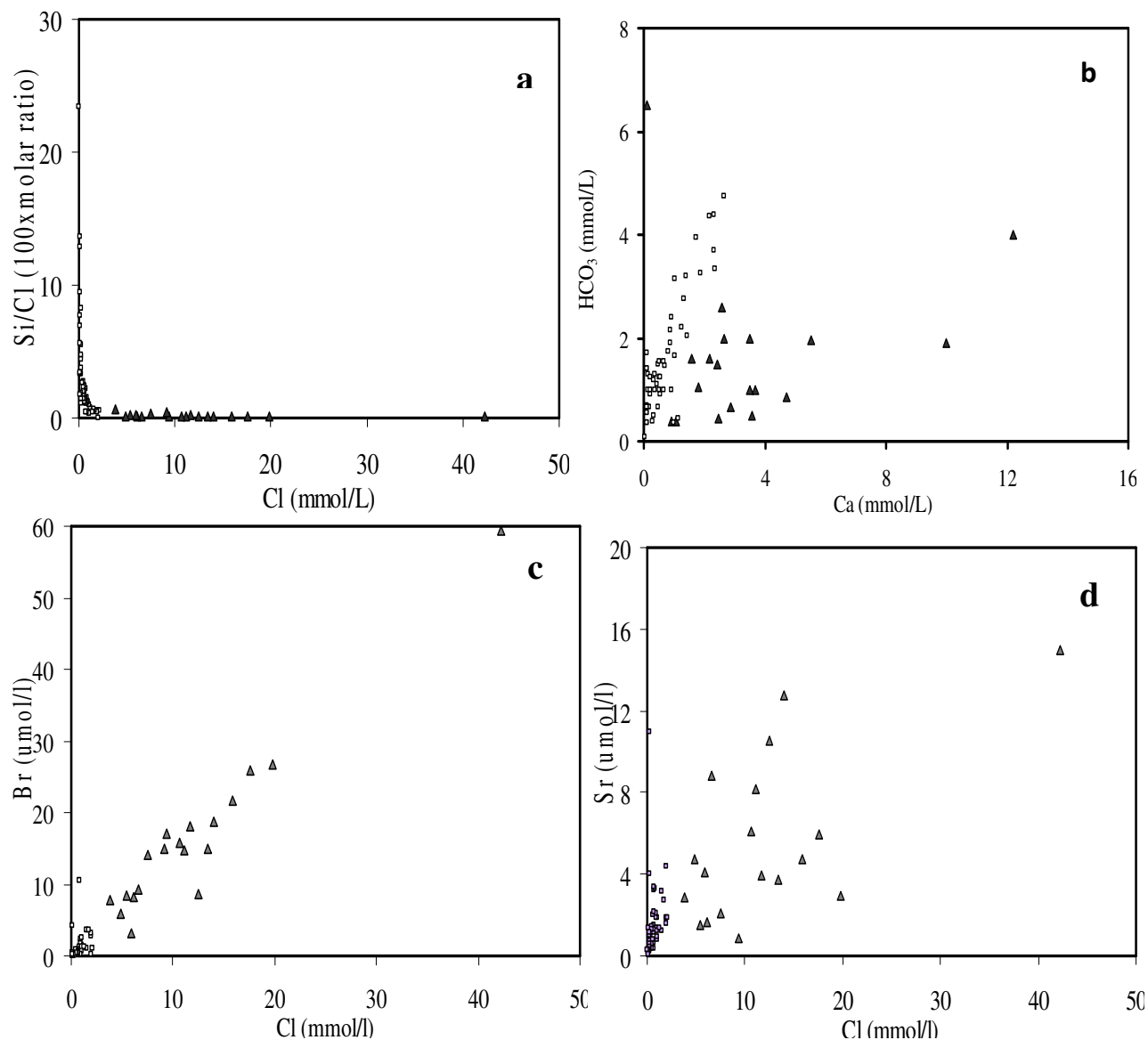
Figure 4. Major and minor ions molar ratios (a) Cl *vs.* Si/Cl, (b) Ca *vs.* HCO₃, (c) Cl *vs.* Br, (d) Cl *vs.* Sr, (empty square: fresh groundwater; filled triangle: saline groundwater).

mechanisms involved are not understood in detail (Mezuman and Keren, 1981; Keren and O'Connor, 1982). By using binary mixing models of B, Na and Ca against the conservative Cl, it has been possible to conceive the relative enrichment/depletion of these ions in terms of desorption/sorption processes, ion exchange reactions which take place respectively in response to freshening and salinization processes in the saline groundwater strip. The mixing phenomenon in terms of flow direction and mixing regime have been thereafter evaluated (Faye et al., 2005).

During this investigation, we did not measure the redox potential neither the dissolved oxygen to clearly shed the occurrence and distribution of the metals in the

groundwater. However, it is clear from the distribution of the redox controlled species that oxidising conditions are maintained within the aquifer. Moreover, the concentrations of nitrate (up to 987 mg/l) are high and indicate that aerobic conditions prevail, since nitrate is rapidly reduced in the absence of dissolved oxygen (Edmunds et al., 1984).

The ranges of values (Figure 6) obtained are: 0 to 132 µg/l Fe; 0 to 971 µg/l Mn; 0 to 1.9 mg/l Ba; 0 to 4.6 mg/l Zn with higher values measured in the Saloum River water samples (10.2 to 23.6 mg/l); 0 to 55 µg/l Cu; and 0 to 105 µg/l Ni; 0 to 3.2 µg/l Cd; 0 to 88 µg/l Co; 0.21 µg/l Cr and 0 to 20 µg/l Pb.

No distinct pattern has been observed between pH and

Table 2. Minor ions and isotopes characteristics of water samples.

N°	Li	Sr	Si	Mn	Fe	Ba	Zn	Cu	Ni	F	Br	B	Cd	Co	Cr	Pb	$\delta^{18}O$	δ^2H	^3H
						µg /l						%							TU
1	3	289	3.6	24	5	426	542	1	11	46	101	64	0.92		3.06	5.22	-5.6	-37	7.2
2	5	22	2.6	11	7	39	45	1	4	21	139	71	0.46		1.95		-5.6	-37	8.2
3	1	9	3.0	1	10	14	26	2	3	103		93	0.71		3.7	1.85	-5.7	-37	1
4	2	30	2.9		7	17	8	1	4	11	55	79	0.6		0.57	5.89	-5.9	-39	5.3
5	8	71	2.9	66	9	413	152	10	25	41	112	62	0.67	10.99	0.54	0.52	-5.8	-39	10.7
6	4	24	3.0	30	11	50	48	2	8	16	28	46	0.7	0.78	2.27	3.69	-5.8	-39	5.9
7	3	26	4.5		13	67	38	2	6		18	60	0.51		1.31	2.07	-5.3	-36	2.6
8	1	88	3.5		3	9	56	1	6	24	6	66	0.72			5.25	-5.4	-36	3.9
9	2	42	3.3		11	16	84	55		133	17	73	0.58		0.91	11.24	-5.4	-36	3.2
10	31	414	4.3	199	6	24	1623	1	1	119	466	159	0.59		0.48	3.19	-4.6	-31	2
11	3	328	9.2		3	20	271	2	2		1200	257	0.85		0.86	4.28	-4.8	-32	2.1
12	3	239	9.2	58	3	268	384	1	3	188	287	66	0.89	1.12	0.46		-5.3	-37	8.5
13	1	27	9.6		2	8	18	1	4	23	27	48	0.53				-5.5	-39	8.7
14	4	34	6.9	19	3	74	44	1	1		39	37	0.4	1.29	0.87	2.88	-5.4	-38	4.4
15	29	771	9.3	603	132	1946	1133	9	97	285	739	46	1.17	88.24	0.01		-5.0	-34	2.1
16	16	278	9.8	465	2	752	825	11	41	80	279	54	0.95	36.47	0.96	2.75	-5.1	-36	4.3
17	1	80	10.2		4	127	98	1	3	156	47	35	0.66		0.91	6.9	-5.7	-40	4.8
18	2	116	7.2		3	168	174	1		36	29	34	0.52				-5.5	-38	2.9
19	2	49	9.3		8	123	115	1			29	38	0.33		5.34		-5.8	-39	0.7
20	6	56	9.4	153	9	304	113	2	23	16	28	28	0.63	20.1	0.23	5.32	-5.7	-38	1.3
21	2	117	12.1	20	2	160	170	1	7		23	93	0.73			5.5	-5.9	-39	1.4
22	1	143	8.4		4	355	450	1	4	120	660	65	0.73	0.02	1.93		-5.6	-37	2.4
23	42	1118	14.7	79	3	1336	1390	2	39	29	1495	69	0.45		1.31	0.59	-5.7	-38	2.4
24	42	1316	25.2	971	6	139	4677	7	39	688	4750	113	3.12	29.27	0.63	5.45	-4.9	-35	2.4
25	6	519	23.4		17	216	1634	1		2006	2066	83	0.74		5.84	2.52	-5.6	-37	2.4
26	109	360	13.9	532	9	671	773	3	43	305	253	54	1.17	27.35	0.49		-5.2	-37	1.7
27		118	9.9		9	213	263	10	2	680	840	45	0.76		2.23		-5.6	-38	0.7
28	1	164	11.2	1	8	250	299	1	3	447	79	48	0.5		2.38	0.25	-5.5	-37	1
28		125	13.9		11	79	231	1		60	31	45	0.61		5.29	8.51	-5.7	-39	1
30	2	53	12.2		11	21	10	1	2	10	24	38	0.47		5.05		-5.8	-40	1.6
31	3	963	15.8		1	28	95	1	1	215	18	52	0.46		1.18		-5.0	-35	1.4
32	2	68	14.1	8	3	73	141	1	4	20	31	44	0.83		0.6	2.28	-5.5	-37	1.2
33	1	109	7.0			147	364	1		31	79	50	0.68			3.49	-5.3	-36	3.6
34	3	25	8.5		3	19	25	1		13	38	31	0.23				-5.5	-38	9.5
35	3	99	14.1		4	80	168	1	2	16	52	29	0.82		0.71	3.85	-5.5	-37	2.2

Table 2. Continued.

36	8	190	7.8	105	6	493	349	3	105	69	39	44	0.31	14.95	1.66	4.95	-5.3	-36	0.8
37	2	17	8.7	58	15	22	46	5		14	18	33	0.74		5.26	2.67	-5.7	-38	0.7
38	2	26	9.3		15	16	19	1				25	0.67		5.62	4.63	-5.9	-39	2.8
39	1	63	8.6	20	14	31	647	7		50	13	26	0.68		1.79	7.52	-6.1	-41	0.9
40	2	36	12.0	57	7	19	32	1	4	1	4	28	0.59		0.81	4.05	-5.7	-38	4.5
41		177	10.9		33	87	353	1	1	203	43	15	0.41		10.81	2.11	-5.8	-40	0.8
42		165	10.6		13	113	189	1		176	105	38	0.64		1.63	1.75	-5.8	-38	3.9
43		136	9.0		74	112	365	1	4	293	251	32	0.85		16.62		-5.8	-39	0.7
44	2	132	8.9		5	234	359	1	3	156	51	28	0.7		0.99	0.99	-5.8	-39	1
45	8	718	11.6	590	1	326	2839	2	60		1180	42	0.7	23.94	0.72	1.94	-5.0	-36	2.2
46		182	9.5		2	215	446	1	1	138	178	15	0.79	0.05	0.26	2.31	-5.8	-39	0.8
47	1	535	10.2	1	2	891	922	1	5		1269	17	0.69			10.09	-5.2	-37	1.3
48	5	293	7.9	50	45	245	312	8		154	71	19	0.63		13.81	6.03	-5.3	-36	5.4
49		923	7.2		17	177	2301	1			687	61	0.78		9.84	2.26	-4.7	-34	3
50	17	164	0.3	73	50	487	640	21	18		220	32	0.64	5.65	15.31		-5.4	-37	5.8
51	3	122	8.7	30	34	43	211	1	5	65	108	27	0.63	2.1	10.4	0.76	-5.5	-37	0.8
52		85	9.6		28	87	284	1		240	27	16	0.47		13.71		-5.8	-39	0.9
53	2	25	9.6	12		33	49	3		72	12	18	0.43	0.4		0.55	-5.8	-39	2
54	2	9	10.9	4	51	2	109	1	2	637	16	7	0.6		13.71	3.76	-5.7	-38	1.3
55	6	113	9.8	71	71	202	234	1	19	1	59	15	0.7	11.59	17.5	1.68	-5.9	-40	5.8
56	2	15	9.3	25	48	13	252	1	2	467	7	12	0.53		16.34	0.66	-5.7	-37	1
57	2	352	12.9			30	83					14	0.68		2.06	0.27	-5.5	-37	3.2
58	18	72	10.4		34	34	160	1	1		1370	650	0.87		10.91	0.83	-6.1	-42	1.1
59	2	415	14.0		20	94	1696	1			1730	78	0.84		6.41	20.47	-5.8	-38	3.3
60		281	10.1			171	499	1	1	21990	61	12	0.69			2.29	-5.7	-40	1.3
61	1	135	12.5		42	331	461	1	7	47	670	13	0.6		14.31	3.81	-5.7	-39	2.8
62	1	163	14.0		50	266	321	1	3	103	158	11	0.53		17.35	0.36	-5.6	-39	1.4
63		108	12.4		47	139	207	1	5	90	207	14	0.64		15.67		-5.5	-39	1.1
64	3	101	12.8		8	159	184	1		50	22	12	0.7		3.7	2.52	-5.7	-38	1.2
65	5	118	20.0	1	84	13	67	1		74	339	23	0.5		21.75	2.84	-5.9	-39	1.4
66	3	381	11.4		31	236	328		1	54	12	25	0.43		9.68		-5.1	-34	2.1
67	14	256	13.6		55	172	278	1	1		2129	31	1.24		21.5	0.55	-5.0	-36	2.8
68	63	185	25.7	332	43	587	338	4	65	175	1129	34	2.6	57.92	14.23		-5.1	-36	3.7
69	18	249	25.1	122	34	511	495	2	31	63	629	31	1.03	20.54	11.85	1	-5.3	-36	5.1
70		6255			2	8	10298					5024					1.7	3	2.4

Table 2. Continued.

71	28	347	27.5	360	67	999	937	13	94	55210	1450	25	1.8	81.35	10.31	0.52	-5.0	-32	3.6
72		6248				6	23683		3	448		9600				1.18	1.5	3	2.4
73		6166										11800					1.5	0	2.6
74			41.7							64680	1195	45					-4.7	-35	4.7
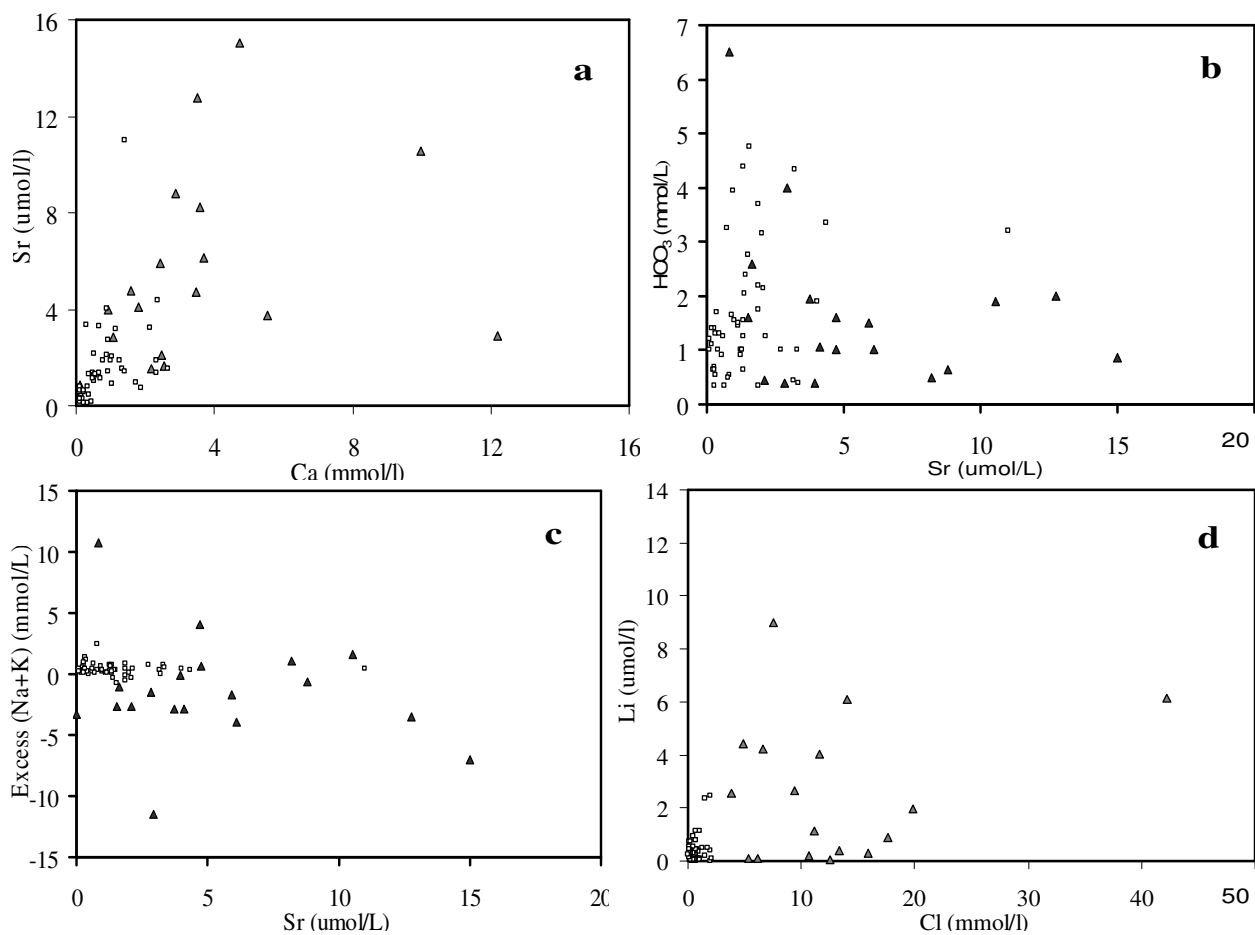
Figure 5. Minor ions molar ratios (a) Ca *vs.* Sr, (b) Sr *vs.* HCO3, (c) Sr *vs.* Ex(Na+K), (d) Cl *vs.* Li (empty square: fresh groundwater; filled triangle: saline groundwater).
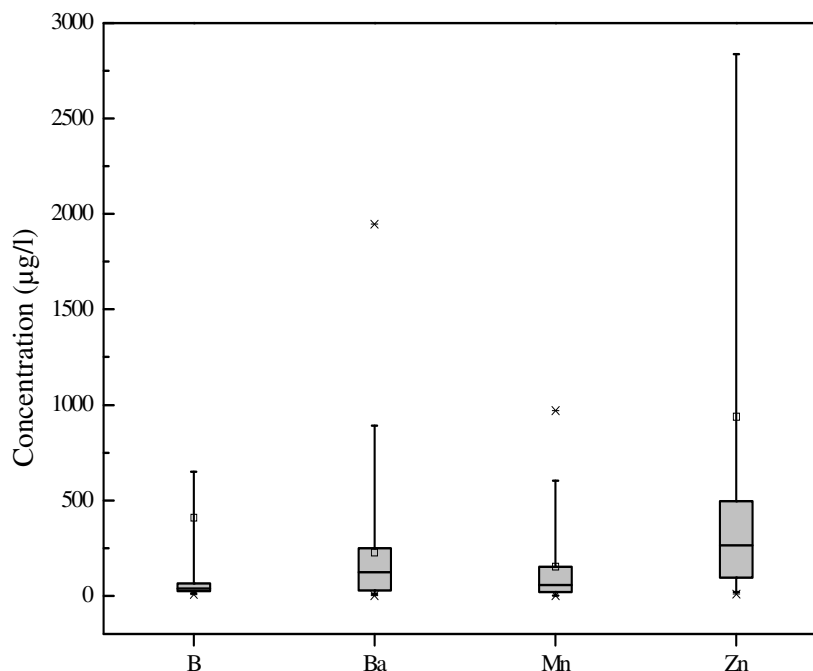
Figure 6. Box plots showing distribution of trace elements.

metals neither metals *vs.* SO$_4$ or Cl concentrations in the groundwaters, although some saline groundwaters metals concentrations can be derived from complexation by Cl which would enhance metal release in solution. This same observation of undistinguished distinct trend across the flow path is noticeable, but it can be seen from the spatial distribution that occurrence of moderate to high concentrations of some of the minor and trace elements (Fe, Ba, Mn, Sr and Zn) are displayed in the northern and western parts of the aquifer and sparsely in the central-eastern zone. These metals and trace elements enrichment is the results of the highly weathering processes of the aquifer matrix evidenced by the occurrence of sparse occurrence of a ferralitic crust, Fe-oxides and hydroxides (goethite being more abundant than hematite) at shallow depth (< 5 m). The highly weathering processes seem even to progressively liberate the Fe contained in the oxides and hydroxides together with the co-precipitated Zn, Mn ions by incongruent reactions from carbonate, silicate or oxide minerals and sorption/desorption reactions. Also the dissolution of the quartz mineral is though to contribute as evidenced by the diagram Si vs.Cl and by the dissolution figures observed in the quartz grains (Lappartient, 1985).

Stable isotopes and tritium

Meteoric and surface waters

The characterization of local meteoric and surface waters

is essential to the deduction of the sources and behaviour of the shallow groundwater flow. In the Saloum system, due to the highly heterogeneous nature of the aquifer together with both temporal and spatial rainfall variability, the recharge mechanism may be complex and discontinuous, and local recharge rate may vary widely. This has been evidenced by early studies (Edmunds, 1990; Gaye, 1990) which used Cl mass balance in the unsaturated zone at Nioro locality where computed recharge rates range from 11 to 108 mm/year. During this present investigation, no rainwater samples were collected and isotopically analysed to characterise the input signature of the stable isotopes and tritium, and thereafter establish the origin, age and evolution of the groundwater, we have used the available rainfall stable isotopes data from Travi et al. (1987), Gaye (1990) and also recent unpublished data year (2007) from Dakar precipitation. These data may be considered as suitable (although most of them are relatively old 1986 to 1989) for this study since they underlined some influence of local oceanic vapour on the Senegalese coast. Moreover, correlations found from the δ^{18}O/ δ^2H pairs are relatively close to the Global Water Meteoric Line (GWML) of Craig (1961). Concerning the ^{3}H content, the lack of record in precipitation in the region permits only a qualitative interpretation. Its presence in the groundwater indicates at least a proportion of water recharged within the last 40 to 50 years. However, approximation of the input signal can be made by using data from Bamako (Mali) (1963 to 1979) and Niamey (Niger) precipitations (1989 to 1994) and the reconstruction of Niger precipitation (Leduc et al., 1996). The present precipitation ^{3}H content would range
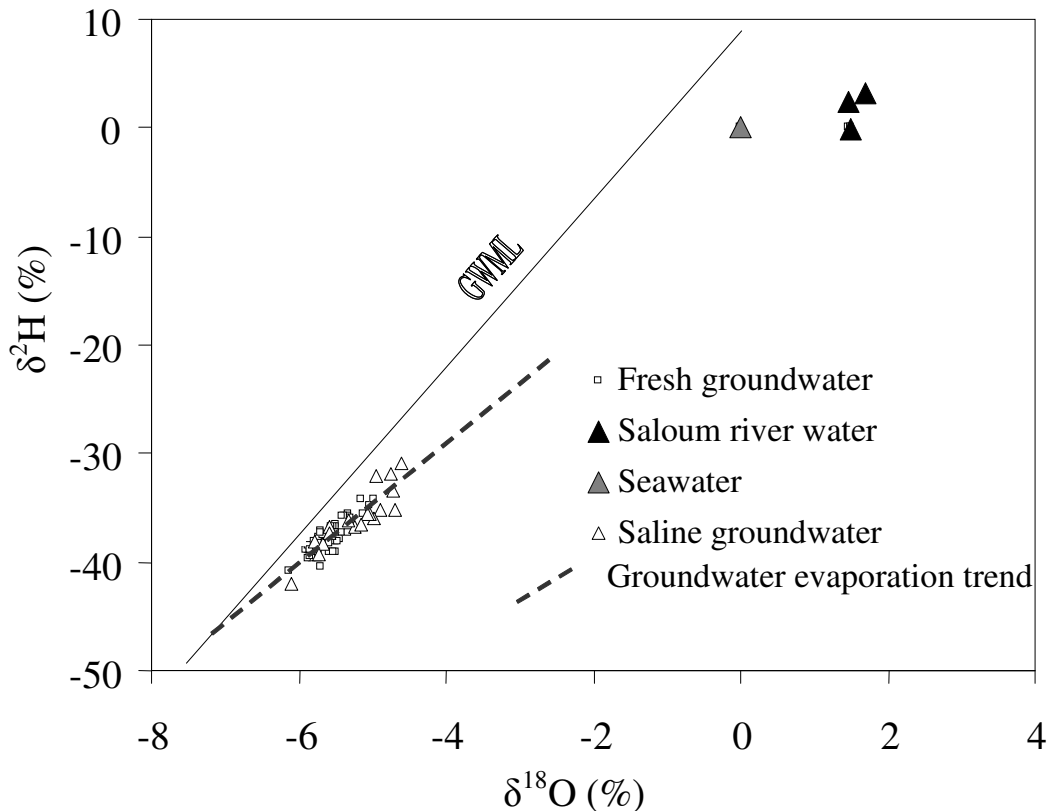
Figure 7. $\delta^{18}O$ / δ^2H diagram

between 2-3 TU, representing a complete removal of the bomb tritium. These values are likely and very consistent with the measured values of 2.4 to 2.6 TU obtained in three locations along the Saloum River and also in Dakar precipitation (1.8 to 2.8 TU). Further, as tritium is a con-servative tracer, changes in content due to evaporation are small relative to measurement errors. The stable isotopes of ^{18}O and ^2H of the Saloum River in these three locations vary in a narrow range; between +1.4 and +1.7% for $\delta^{18}O$, and between -0.1 and +3.1% for δ^2H. This small enriched isotopic range may indicate a mixture of the stagnant intruded saline water with water derived from precipitation on lower catchment slopes. Analysis of the major-ion chemistry and EC values (Table 1) of the Saloum River water in these three locations which exhibits higher mineralisation compared to seawater values reflect a little contribution of the precipitation to dilute the stagnant intruded saline water. Note that these data were collected after the rainy season and are enriched in $\delta^{18}O$ and δ^2H due to the high evaporation rate prevailing in this region.

Stable isotopes and tritium in the groundwater

By plotting $\delta^{18}O$ against δ^2H data of the groundwater, a distinguished trend is identified with scattered line of Y =

5.5X - 8.7 (R^2: 0.98; slope: 5.5). They display values ranging between -6.1 and -4.6% for $\delta^{18}O$ and between -42 and -31% for δ^2H (Figure 7).

Through spatial distribution analysis of the isotope data (Figure 8), it can be seen from the system, ^3H values are variable from less than 2 TU to 10.7 TU with narrow stable isotopes values (-6 to -5%) in the piezometric mound region; this likely indicates a recharge area where groundwater renewability is likely variable depending on the sites conditions e.g. ground topography and slope, depth to water table, soils characteristics. Piston flow type and perhaps preferential flow recharge mechanism seem to be prominent to account for the variability in ^3H content within this narrow area. This is consistent with the highly variable recharge values found in the Saloum using CMB method (Edmunds and Gaye, 1994). The lighter stable isotopes ($\delta^{18}O$ < -6.0%) values and ^3H less than 2 TU are observed through the active groundwater flow zone located in the centre of the aquifer down to the groundwater trench area; in this region, mixing between sub modern and recent recharge water seems to be the most likely process which would alter the ^3H content below present day input value. In contrast, in the west and north at the vicinity of Saloum River, groundwater is characterised by depleted $\delta^{18}O$: -6 to -5% and ^3H between 2 to 2.5 TU. Present recharge seems to be the prominent together with mixing during regional flow.
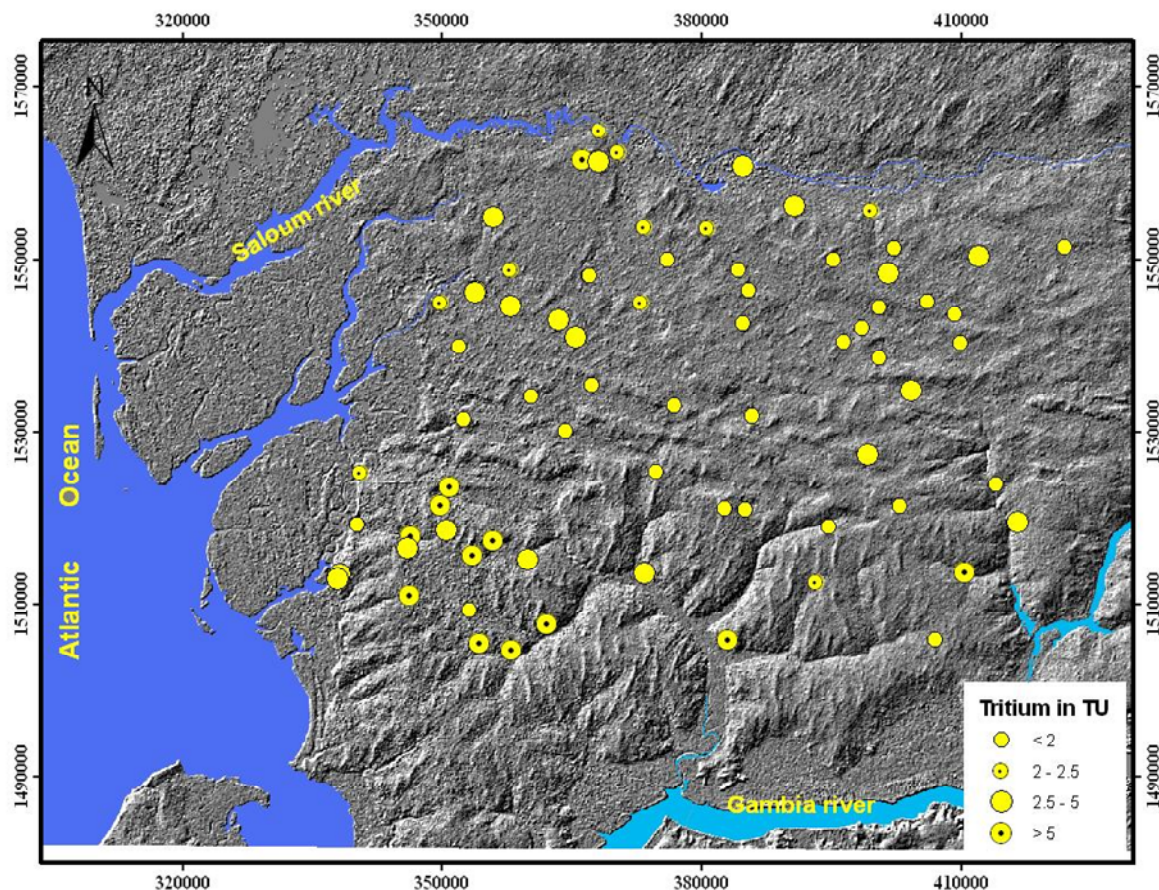
Figure 8. ^{3}H content distribution map.

Conclusion

A combined interpretation of hydrochemical, isotope and hydrodynamic data gathered from the Saloum aquifer has enabled to constrain the main geochemical processes and to feature several aspects of the groundwater flow regime. The common conservative ions Cl and Br *vs.* major, minor and trace elements, and saturation index of specific minerals were mainly considered to shed the likely geochemical reactions taking place in the system. The overall hydrogeochemical and mineralization trend found reflects: (1) active water rock interaction involving both congruent/incongruent mineral weathering and ion exchange reactions; (2) admixture with intruded saline surface water in the western and northern limits of the system and (3) both recharge and discharge by evaporation in this highly inhomogeneous system within the context of a semi-arid climate.

The water types previously defined (Faye et al., 2005) according to the dominant ions and their mineralization, and independently to their possible alterations related to the age and possible recent recharge are considered in a consistent picture of the origin and age of water as well as the sources of the main components. Evidences are provided by minor, trace elements chemistry and isotope

data together the mineralogy aquifer matrix and the hydrodynamic data. At the piezometric mound, the occurrence of low to moderate mineralised Na-HCO$_3$ and Na-Cl waters which correspond to the highest tritriated groundwater in the system reflect ion-exchange processes (where Ca replaces Na on the exchanger sites of the clay minerals) since primary minerals such as feldpar and micas are absent in the mineralogy phase. Moreover, excess (Na+K) *vs.* dissolved Sr plots militates against weathering of these primary minerals. The Cl content increase in some samples located in this area is accompanied by an increase in NO$_3$ concentrations; this trend confirms the hypothesis that NO$_3$ is extremely stable ions in aerobic conditions just as conservative Cl (Appelo and Postma, 1994). Towards the eastern and central parts of the aquifer, the dominantly Ca-HCO$_3$ waters together with the positive correlation between Ca and HCO$_3$ and the SI$_{calcite}$ values suggest that carbonate dissolution is somewhat a major process. But it is shown that many of the solutes (Fe, F, Ba, Mn, Sr and Zn) are derived in addition to carbonate dissolution, at least in part, from incongruent reactions from silicate or oxide minerals and sorption/desorption reactions. The stable isotope and tritium contents imply that the groundwater in these areas was derived from recent precipitation. These

incongruent dissolution and sorption/desorption reactions which produce high minor and trace elements occur predominantly in the higher chlorinity Na-Cl and Na/Ca-Cl water types originating from mixing with the saline Saloum River water. In these areas, the relatively enriched waters (δ^{18}O: -5.2 to –4.6%) and ^{3}H contents (2 to 5 TU) reflect both recharge and discharge by evaporation.

ACKNOWLEDGEMENTS

REFERENCES

Adar EM, Neuman SP (1988). Estimation of spatial recharge distribution using environmental isotopes and hydrochemical data II. Application to Aravaipa Valley in Southern Arizona, USA. J. Hydrol., 156:47-59.

Agrawal V, Vaish AK, Vaish P (1997). Groundwater quality: focus on fluoride and fluorosis in Ragasthan. Curr. Sci., 73(9):743-746.

Appelo CAJ, Postma D (1994). Geochemistry, groundwater and pollution, 2nd edn., Balkema, Rotterdam, The Netherlands.

Arad A, Kafri U, Halicz L, Brenner I (1986). Genetic identification of the saline origins of groundwaters in Israel by means of minor elements. Chem. Geol., 55(3-4):251-270.

Coleman ML, Shepherd TJ, Durham JJ, Rouse JE, Moore GR (1982). Reduction of water with zinc for hydrogen isotope analysis. Anal. Chem., 54: 993-995.

Conrad G, Lappartient JR (1987). The "Continental terminal"; its position within the Cenozoic geodynamic evolution of the Senegalo-mauritanian basin. J. Afr. Earth Sci., 6(1):45-60.

Craig H (1961). Isotopic variations in meteoric water. Sciences, 133: 1702-1703.

Darling WG, Edmunds WM (1987). Geochemistry of saline waters in sedimentary basins in the United Kingdom. Investigation of the Geothermal Potential of the UK. Report, British Geol. Surv., London.

Diluca C (1976). Hydrogeology of the Continental terminal aquifer between the Sine and the Gambia. Technical report, BRGM DKR 76 DK (in French).

Diop ES (1986). Tropical holocen estuaries. Comparative study of the physical geography features of the rivers from the south of Saloum to the Mellcorée (Guinea Republic). PhD, Université L Pasteur Strasbourg (in French).

Dror G, Ronoen D, Stiller M, Nishri A (1999). Cl/Br ratios of Lake Kinneret, pore water and associated springs. J. Hydrol. 225:130-139.

Edmunds MW (1990). Groundwater recharge in Senegal. Technical Report British Geological Survey, WD/90/49R.

Edmunds WM, Cook JM, Miles DL (1984). A comparative study of sequential redox processes in three British aquifers. In: Eriksson E (ed) Hydrochemical Balances of Freshwater systems, IAHS Publ., 150: 55-70.

Edmunds WM, Carrillo-Rivera JJ, Cardona A (2002). Geochemical evolution of groundwater beneath Mexico City. J. Hydrol 258:1-24.

Edmunds WM, Gaye CB (1994). Estimating the spatial variability of the groundwater recharge in the Sahel using chloride. J. Hydrol., 156: 47-59.

Edmunds WM, Smedley PL (2000). Residence time indicators in groundwater: the East Midlands Triassic sandstone aquifer. Appl. Geochem., 15: 737-752.

Edmunds WM, Walton NRG (1980). A geochemical and isotopic approach to recharge evaluation in semi arid zones; past and present. In: Fontes JC (ed) Arid-zone hydrology, investigation with isotope techniques. Int. Atomic Energy Agency, Vienna, pp. 47-68.

Epstein S, Mayeda TK (1953). Variations of ^{18}O content of waters from natural sources. Geochem. Cosmochim Acta, 4: 213-224.

Faye S, Cissé Faye S, Ndoye S, Faye A (2003). Hydrogeochemistry of the Saloum (Senegal) superficial coastal aquifer. Environ. Geol., 44: 127-136.

Faye S, Maloszewski P, Stichler W, Trimborn P, Cisse Faye S, Gaye CB (2005). Groundwater salinization in the Saloum (Senegal) delta aquifer: minor elements and isotopic indicators. Sci. Total Environ., 343: 243-259.

Gaye CB (1990). Isotopic and geochemical investigations of the recharge and discharge mode in the semi arid northern Senegal unconfined aquifers. PhD. C. A. Diop University, Senegal.

Ghassemi F, Jakeman AJ, Nix HA (1995). Salinization of land and water resources : human causes, extent, management and case studies. Univ. New South Wales Press, Sydney, Australia.

Keren R, O'Connor GA (1982). Effect of exchangeable ions and ionic strength on boron adsorption by montmorillonite and illite. Clays Miner., 30: 341-346.

Lappartient JR (1985). The Continental terminal and the early Pleistocene of the Senegalo-mauritanian basin. Stratigraphy, sedimentology, diagenesis, alterations, paleoshore reconstitutions from the ferralitic formations, PhD University Marseille, France.

Leduc C, Taupin JD, Le Gal LaSalle C (1996). Estimation de la recharge de la nappe phréatique du Continental terminal (Niamey, Niger) à partir des teneurs en tritium. C R Acad. Sci. Paris, serie IIa, 315: 599-605.

Lee ES, Krothe NC (2001). A four-component mixing model for water in a karst terrain in south-central Indiana, USA. Using solute concentration and stable isotopes as tracers. Chem. Geol., 179: 129-148.

Mezuman U, Keren R (1981). Boron adsorption by soils using a phenomenological adsorption equation. Soil Sci. Soc. Am. J., 45: 722-726.

Richter BC, Kreitler CW (1993). Geochemical techniques for identifying sources of groundwater salinization. CRC Press, Boca Raton.

Thatcher LL, Janzer VJ, Edwards RW (1977). Methods for determination of radioactive substances in water and fluvial sediments. In: Techniques of Water Resources Investigations of the US Geological Survey, US Government Printing Office, Washington.

Travi Y, Gac JY, Fontes JC, Fritz B (1987). Chemical and isotopic survey of rain waters in Senegal. Géodynamique, 2(1): 43-53.

Uliana MM, Sharp Jr JM (2001). Tracing regional flow paths to major springs in Trans PecosTexas using geochemical data and geochemical models. Chem. Geol., 179: 53-7.